THESIS FOR THE DEGREE OF LICENTIATE OF ENGINEERING IN THERMO AND FLUID DYNAMICS

TOWARDS VALIDATED CATALYTIC REACTOR MODELS

MAGNUS WALANDER

Department of Mechanics and Maritime Sciences
CHALMERS UNIVERSITY OF TECHNOLOGY
Gothenburg, Sweden 2020

TOWARDS VALIDATED CATALYTIC REACTOR MODELS
MAGNUS WALANDER

Thesis for the degree of Licentiate of Engineering 2020:04
Division of Combustion and Propulsion Systems
Department of Mechanics and Maritime Sciences
Chalmers University of Technology
SE-412 96 Gothenburg
Sweden
Telephone: +46 (0)76-833 53 20

Cover Picture: Illustration of length scales involved in a diesel oxidation catalyst.

Chalmers Reproservice
Gothenburg, Sweden 2020

Abstract

The use of liquid fuels in the internal combustion engine inherently produces several toxic emissions that need to be removed. This is done through a series of catalytic converters, referred to as the exhaust aftertreatment system (EATS), each catalyst with its own purpose. To cope with increasingly stringent emission legislation for the automotive industry, the performance of these catalysts needs to improve. For their development, modelling is an indispensable tool.

This thesis presents a mathematical model, a so-called single-channel 1+1D reactor model, that describes the reactions that occur inside a diesel oxidation catalyst (DOC) - along with the heat and mass transport. Moreover, the purpose was to improve an already existing model using relevant experiments such as kinetic experiments in a synthetic catalyst activity test (SCAT) bench, gravimetric analysis (GA), temperature programmed desorption (TPD) as well as scanning electron microscopy (SEM). These experiments enabled better inputs for the modelling framework. Furthermore, emphasis has been put towards investigating boundary conditions for the experimental setup. The radial mixing in a SCAT bench was investigated using pair of cleverly designed DOCs. The investigation showed that there was a concentration maldistribution across the catalyst inlet and the problem was solved using a 3D printed α-alumina mixer.

The original 1+1D model relies on some simplifications which are rarely fulfilled. The model assumes that the catalytic washcoat forms a uniform slab - an assumption which may lead to incorrectly estimated light-off temperatures. This limitation of the 1+1D model was circumvented through the use of a sectionalizing principle, where the washcoat was divided into multiple segments which were simulated independently. Different experiments allowed for estimation of local properties - such as external mass transfer coefficient, washcoat porosity and thickness. The new model showed increased NO conversion at elevated temperatures compared to the original model.

By improving these single-channel models, EATS modelling in general can become more predictive - leading the way to emission-free transportation.

Keywords: Exhaust aftertreatment modelling, EATS, diesel oxidation catalyst, synthetic catalyst activity test, scanning electron microscope, gravimetric analysis, effective diffusivity, washcoat

List of publications

This thesis is based on the work contained in the following publications:

Publication I M. Walander, A. Nygren, J. Sjöblom, E. Johansson, D. Creaser, J. Edvardsson, S. Tamm and B. Lundberg. "Use of 3D-printed mixers in laboratory reactor design for modelling of heterogeneous catalytic converters."
Submitted to Chemical Engineering and Processing: Process Intensification

Publication II M. Walander, J. Sjöblom, D. Creaser, B. Lundberg, S. Tamm and J. Edvardsson. "Efficient Experimental Approach to Evaluate Mass Transfer Limitations for Monolithic DOCs."
in Topics in Catalysis (2019) Vol. 62, 1–4, p. 391–396.

Publication III M. Walander, J. Sjöblom, D. Creaser, B. Agri, N. Löfgren, S. Tamm, J. Edvardsson and I. Hitchcock. "Modelling of mass-transfer resistances in non-uniformly washcoated monolith reactors."
Submitted to Emission Control Science and Technology

Acknowledgements

First of all, I would like to thank my supervisors Jonas Sjöblom and Derek Creaser for giving me the opportunity to work on this project, for guiding me through solving problems and for helping me to create new ones. Our Friday morning meetings have kept me motivated through these two and a half years.

Secondly, I would like to extend my gratitude to several project members. To Björn Agri for helping me with and providing the reactor code, to Stefanie Tamm, Jonas Edvardsson and Niklas Löfgren for helping me plan experiments and perform industry relevant research. I would also like to thank and apologize to Mats Mannhem, Anna-Lena Lindahl, Iain Hitchcock and Nadezda Sadokhina for helping me performing excellent but sometimes extremely tedious experiments at Johnson Matthey. Funding from the Swedish Energy Agency is gratefully acknowledged.

Many thanks to my lovely coworkers at the division of Combustion and Propulsion Systems - I may not work with engines but that does not mean we cannot be friends. Especially, thanks to Marco Fistler for literally dragging me to the *fika* table when I felt I didn't belong.

I would also like to thank my mother Anki, brother Tomas and father Mats. I would never have gotten this far in life without your endless support. Huge thanks to my oldest friend Emil Johansson for 3D printing cool tools for our project and being my friend.

Last but no least, I would like to thank my closest friend in the world - Anna. Your full-sized aortic pump and smile have helped me through many tough times and you have always motivated me to keep fighting. Thank you for also teaching me that there are other things in life apart from my PhD project - though sometimes it takes a while to understand a lesson. Lastly, a sort of thank you to Nelson the cat for biting my toes in the morning - forcing me to get to work.

Contents

1 Introduction

This chapter will provides a brief overview of why automotive converters are needed, the basic principle for exhaust aftertreatment along with the objectives of this thesis.

1.1 Environmental and health aspects

The incomplete combustion of liquid or gaseous fuels in the internal combustion engine (ICE) inherently produces small but significant concentration of carbon monoxide (CO), unburnt hydrocarbons (HC) and particulate matter (PM). Furthermore, due to the high temperatures and excess O_2 and N_2, mainly nitrogen monoxide (NO) but also nitrogen dioxide (NO_2) are formed [1]. Lastly, some unique substances may form during combustion depending on fuel impurities - however, their impact can be reduced by having more stringent fuel quality legislation - e.g. SO_2 emissions from road transportion in the European Union (EU) decreased by 99% between 1990 and 2011 following *Directive 98/70/EC* [2].

These emissions are all harmful to the environment or human health. First off, CO poisoning is likely responsible for more than half of all fatal poisonings world-wide, where roughly 70% of the cases are due to exposure to vehicle exhaust [3]. PM is the emission that has been most clearly linked to premature deaths. For example, the World Health Organization (WHO) estimated that the deaths of 3 million people in 2012 were attributable to outdoor air polluted with particulate matter - to which the transportation sector is accountable for roughly 30 and 50% in European cities and OECD countries, respectively [4]. Exposure to PM can lead to lung cancer, chronic respiratory or cardiovascular diseases [5]. Many of the unburnt hydrocarbons are by themselves carcinogenic [6]. Moreover, HC in combination with NO_2 may produce ground-level (tropospheric) ozone (O_3), which is a strong oxidizing irritant [7]. Lastly, NO_X cause acidification of ecosystems and inhalation may cause respiratory problems [8].

1.2 Emission legislation

In 1960s' Los Angeles, the average tailpipe emissions were typically 9 g HC/km, 56 g CO/km 4 g NO_X/km [7]. In combination with these high emissions, temperature inversions would trap the polluted air in the Los Angeles valley and during peak sunlight intensity a strong irritant was present in the city. The concentration of this oxidant correlated well with the sunlight intensity throughout the day - and so it was established that it was troposherpical O_3 that was formed from the polluted air. This problem became a major health concern in some American cities and to reduce this problem the 1970 Clean Air Act was signed [9]. The same year in Europe, Directive 70/220/EEC, would become the foundation for the amendments that created the so-called *Euro Emission Standards*, which restricted the amount of emitted *gaseous pollutants* - at that time only carbon monoxide and hydrocarbons [10].

The Euro Emission Standards have since been revised to gradually reduce the permitted emission levels for different engine types and vehicle classes. These emission levels, between 1993 and 2021, are presented in figure 1.1. Since the legislation for HC and NOx changed between Euro 2 and Euro 3 for respective fuel type, the sum for HC and NOx is shown here. The year on the x-axis corresponds to the year for registration of new vehicles. Note that light duty is judged based on g/km while heavy duty is based on g/kWh. However, the heavy duty emissions levels can be recalculated (using the US HDD truck fleet fleet average of 1.68 kWh/km [11]), arriving at roughly the same emissions levels per km of travel.

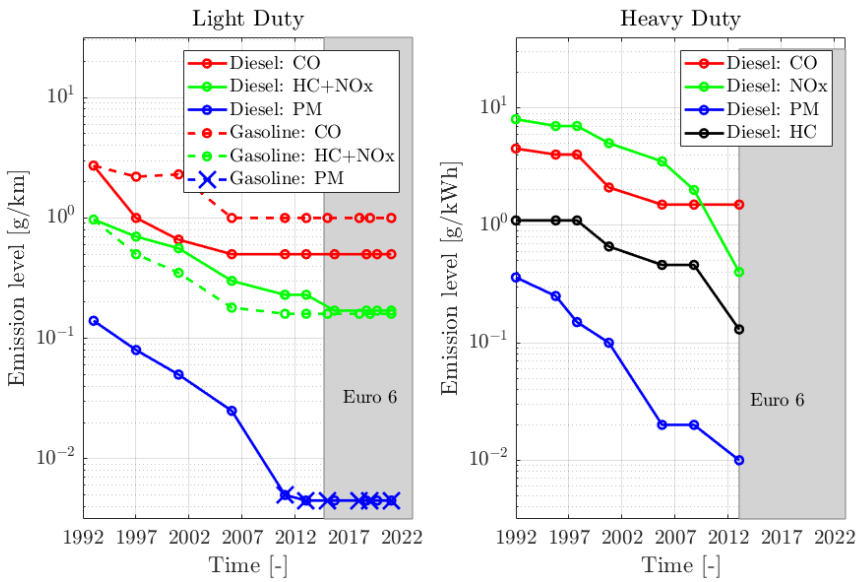

Figure 1.1: *Euro Emission Standard levels between 1992 and 2020 for different fuels and vehicle classes (left - light duty, right - heavy duty).*

1.3 Exhaust aftertreatment systems for diesel engines

Once the automotive industry realized that engine modifications alone could not meet the requirements of the 1970 Clean Air Act, various catalytic systems were investigated. However, aftertreatment for engines is very different from - and much more complex than for example that of a steady-state operated chemical plant process [12]. The exhaust aftertreatment system (EATS) must function at very low temperatures, be able to handle thermal shocks and resist high temperatures, flow pulsations and tolerate various common catalysts poisons (e.g. SO_2). The EATS itself is also prone to vibrations [7]. Lastly, the catalyst itself consists of a noble metal - which is some of the most expensive substances on earth and its use should therefore be minimized. This thesis is heavily focused on the diesel oxidation catalyst, therefore only a modern diesel engine EATS is presented here.

A typical setup for a diesel engine exhaust aftertreatment system is shown in figure 1.2 (red, crossed out substances are removed for each catalyst). The Diesel Oxidation Catalyst's (DOC) main function is to oxidize (the excess O_2 being the oxidant) HC into CO_2 and H_2O, CO into CO_2 and lastly NO into NO_2, which in itself is actually more harmful than NO [1]. However, equimolar ratios of NO and NO_2 will lead to a different and faster reaction mechanism in the Ammonia Selective Catalytic Reduction ($NH_3 - SCR$) catalyst [13]. The DOC also functions to generate an exotherm for active regeneration of the Diesel Particulate Filter (DPF) via e.g. in-cylinder post injection to increase HC concentration [14].

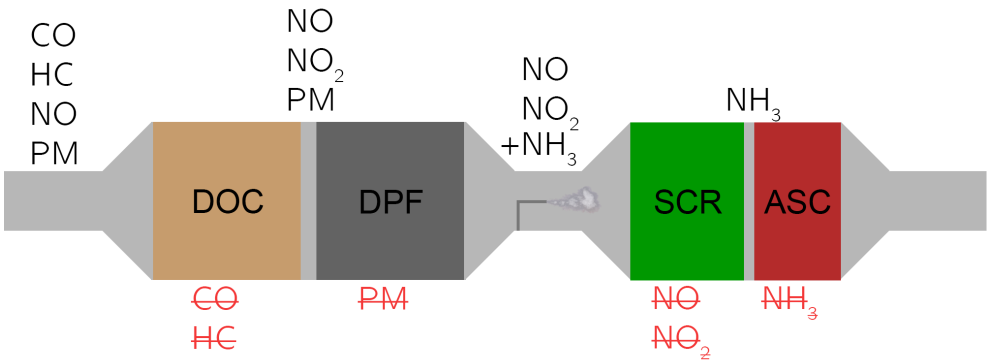

Figure 1.2: *Common components in a modern diesel engine exhaust aftertreatment system.*

The DPF's purpose is to trap and ultimately oxidize PM into CO_2. The Continuously Regenerating Trap (CRT) uses NO_2 created by the DOC and shows significant conversion already at around $300°C$ while the filter that relies on O_2 as oxidizing agent need temperatures above $550°C$ - thus active regeneration is sometimes necessary [15]. Modern variations of the DPF incorporate DOC functionality into the filter walls to reduce thermal mass - i.e. less energy is required to heat less mass of catalyst to get it functioning. This also lowers potential HC or CO slip from the DPF during active regeneration [1]. The third component deals with NO_X abatement. Common catalysts include the $NH_3 - SCR$, the Lean NOx Trap (LNT) and the NOx Storage and Reduction (NSR) - either one of them or in a combination of two (e.g. NSR-SCR). For $NH_3 - SCR$, urea ($CO(NH_2)_2$) is injected upstreams the catalyst to later thermally decompose into NH_3 and CO_2 [16]. NH_3 then reduces NO_X into N_2 and H_2O [1]. Finally, to account for potential overdosage of urea, an ammonia-slip catalyst (ASC) is placed after (or in combination with) the SCR to remove unreacted NH_3 [17].

1.4 Objectives

This thesis focuses on mathematical modelling along with relevant experiments. Experiments procedures include laboratory-scale synthetic catalyst activity tests (SCAT), scanning electron microscopy (SEM) analysis and intelligent gravimetric analysis (IGA). The DOC was chosen since its kinetics are a lot simpler than for example that of the $NH_3 - SCR$, but the findings could easily be extrapolated to different catalyst types, e.g. the three way catalyst (TWC) commonly found in gasoline vehicles [7]. Once sufficient experimental procedures have been established, the project will move over to full-scale catalysts using engine test benches.

The objective of this thesis is to combine relevant experiments and modelling to distinguish mass transfer from kinetics. By separating these phenomenon, the models will be more accurate and therefore predictive - a very important feature for exhaust aftertreatment systems development. The models are also commonly used by the automotive industry to predict the EATS reacts to gear changes, sharp transients etc.

2 Background

This chapter will introduce some fundamental concepts of catalysis along with mathematical modelling of monolith reactors in general, thus distinguishing from next chapter which is solely focused on the reactor model used in this thesis along with analysis and description of experiments.

2.1 History of Catalysis

In Jöns Jacob Berzelius' yearly review of the entire physics and chemistry society from 1835, he stated [18] (translated from Swedish):

> "It is, then, proved that several simple or compound bodies, soluble and insoluble, have the property of exercising on other bodies an action very different from chemical affinity. By means of this action they produce, in these bodies, decompositions of their elements and different recombinations of these same elements to which they remain indifferent."

This is indeed the very first definition of a catalyst - something (bodies) that will enable a reaction to take place (produce decompositions of their elements and different recombinations) while not being consumed itself (remain indifferent). Berzelius called this action "catalysis", from Greek "$\kappa\alpha\tau\alpha\lambda\acute{\upsilon}\omega$" meaning to loosen or to destroy. At the time it was far from understood what part of the chemical reaction that catalysts contribute to or alter. Some suggested that the metallic catalysts was only a mere heat source [19]. However, one early paper from Humphry Davy [20] suggested that a chemical reactions between two gaseous reactants (coal gas and oxygen) only occurs on specific metallic surfaces (e.g platinum), thus proving that the surface itself had additional important properties aside from its temperature.

Two hundred years later and roughly 90% of the products in the chemical industry are produced by means of some catalytic process. Still, the use in practical catalysis outgrows its fundamental understanding - however, many practical concepts helps us understand its basics [21].

2.2 Basics of Catalysis

By now, catalysts are defined by their ability to accelerate a chemical reaction through providing an energetically far superior reaction path compared to its non-catalytic counterpart [21]. Figure 2.1 shows the catalytic oxidation of CO by O_2; as a potential energy diagram and as a typical reaction mechanism. The uncatalyzed (red curve) requires high amounts of energy to produce a gas phase reaction whereas the catalyzed version (green curves) is a lot more favourable. However, the overall change in free energy is identical regardless if a catalyst is being used - the catalyst only changes the kinetics while thermodynamics and also equilibrium are unaffected. The reaction mechanism includes

adsorption of CO and adsorption and dissociation of O_2 in the first step. The adsorbed CO and O then forms adsorbed CO_2 which either desorbs or decoposes back.

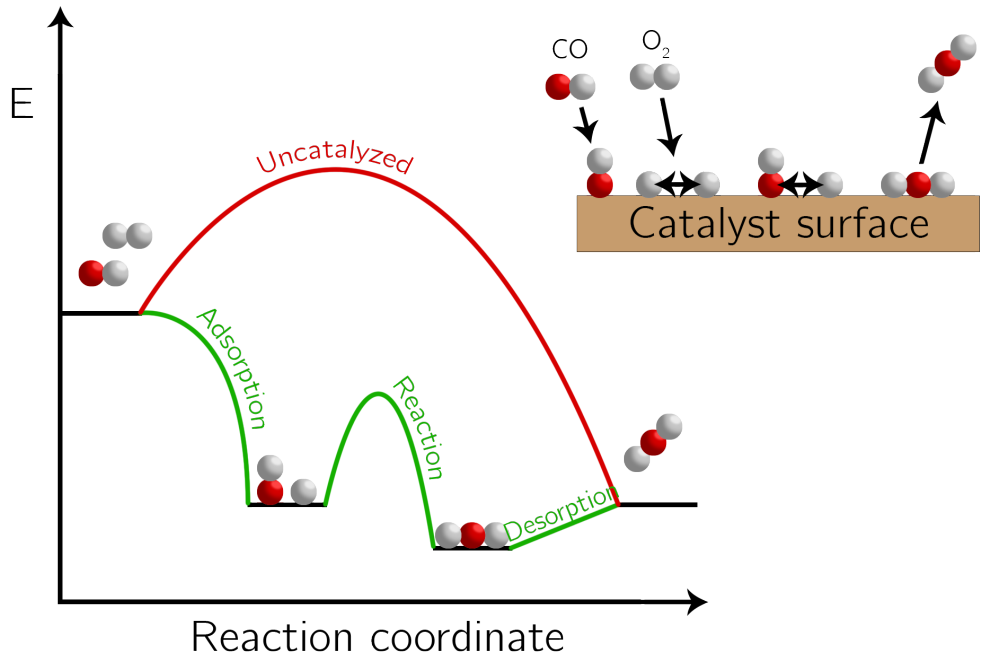

Figure 2.1: *Left: Potential energy diagram of a typical heterogeneous catalytic reaction. Right: Reaction mechanism of CO oxidation by O_2.*

As a consequence of the energetically favourable reaction path, industrial processes can operate at greatly reduced temperature and pressure. Furthermore, the catalyst design can be catered to increase selectivity (the ratio of desired to undesired products) towards a certain product - thus maximizing yield and potentially reducing the need for costly separations in industrial processes [21].

2.2.1 Heterogeneous catalysis

Catalysts comprise anything from atoms and molecules to complex enzymes and surfaces. However, this thesis only deals with heterogeneous catalysis - where the catalyst is a solid which catalyzes molecules in gas phase. Different noble metals are suitable for different oxidation reactions, where according to the Sabatier principle, optimal catalytic performance is achieved where the interaction between reacting species and the noble metal itself is "just right" [21]. If the bonding is too weak neither reactants will stay long enough on the surface to dissociate. On the other hand, if either of the required reactants or final products bond to strongly to the surface, the catalyst will end up getting poisoned and the reaction will die out. The interaction depends on the electron orbitals

of the reactants and the metal, hence different transition metals are suitable for different reactions. Of course, catalyst price and susceptibility towards other poisons that might be prevalent in the inlet feed have to be considered as well [21].

As Humphry Davy established early on, in heterogeneous catalysis noble metal surface area is key. Since the surface area to volume ratio goes up as the particle diameter approaches zero, the smallest possible particles are desired. Additionally, to further improve the accessibility of the catalyst, the particles are typically dispersed in a highly porous material - commonly referred to as a washcoat, where $\gamma - Al_2O_3$ is the most common washcoat material used in automotive converters [21]. The washcoat typically has an extremely high specific surface area of around $150 - 175 m^2/g$ because of its complex pore structure [21]. As a consequence of its high porosity the washcoat is very fragile and is therefore further applied onto a supporting body. In steady-state operated chemical plants this could be a packed-bed reactor while for automotive converters this is most likely a monolith reactor.

2.3 Monolith reactors

Monolith reactors, also known as honeycomb monoliths, comprise a large number of axially parallel channels of an arbitrary shape (yet square channels are most common) [22]. They are used in a wide range of processes due to their compact nature and as a consequence of the highly structured design and small hydraulic diameter the flow is laminar. This leads to a low pressure drop which, in the automotive industry, is important for reducing fuel consumption and maintaining high power output. The monolith reactor has excellent heat transfer properties since it is usually ceramic, as can be seen in figure 2.2, or metallic [22] and typically has 400 cells per square inch (CPSI).

Figure 2.2: *Photograph of a 400 CPSI ceramic monolith placed inside a metal canning.*

However, one problem with monolith reactors is that once the reactants enter the structured channels it is not possible to change any potential concentration maldistributions across channels that e.g. arise from liquid injection of urea upstream the $NH_3 - SCR$ [23]. This can lead to lowered NO_X conversion and increased NH_3 slip. An emerging technology to solve such a problem is the periodic open cellular substrates (POCS) [24] which, at the cost of increased pressure drop, has improved radial heat and mass transfer. However, as of now, the monolith reactor is the state-of-the-art technology for supporting oxidation catalysts in the automotive industry [22]. Its operation occurs in a wide range of flow rates, temperature and concentrations. To characterize the operation for understanding of limiting factors, one may resort to using classical timescales [25]:

$$t_c = \frac{l}{v} \quad t_{td} = \frac{R_{bulk}^2}{D_{AB}} \quad t_{wd} = \frac{R_{wsc}^2}{Deff} \quad t_r = \frac{1}{k_j} \tag{2.1}$$

where $t_c[s]$ is the residence time, $l[m]$ is the channel length, $v[m/s]$ is the average channel velocity, $t_{td}[s]$ is the timescale for transverse diffusion in the open channel, $R_{bulk}[m^2]$ is the characteristic dimension of the open channel, $D_{AB}[m^2/s]$ is the free molecular diffusivity, $t_{wd}[s]$ is the timescale for washcoat diffusion, $R_{wsc}[m^2]$ is the characteristic dimension of the washcoat, $Deff[m^2/s]$ is the effective diffusivity in the washcoat, $t_r[s]$ is the reaction timescale and $k_j[s^{-1}]$ is the reaction rate constant. By relative comparison with the timescale for reaction, one can conclude whether the conversion is limited by residence time (t_c), external mass transfer (t_{td}) or internal mass transfer (t_{wd}).

2.4 Mathematical modelling of monolith reactors

In gaining better fundamental understanding of catalyst performance, modelling can be a valuable tool. There have been huge efforts towards development of mathematical models of monolithic catalytic reactors [22, 26, 27], with a lot of attention on the diesel oxidation catalyst (DOC) with varying degrees of complexity [1, 22, 28, 29]. Due to the vast range of scales (0.1 m to 1 nm) of processes occurring in a monolith reactor, several common simplifications are made to reduce computational cost. The extent of the simplifications depend on the purpose of the application - e.g. is it to model micro-flow in a single washcoat pore or to look at temperature profiles across the entire reactor? The assumptions affect dimensionality of the problem as well as the governing equations - regardless, some simplifying assumption regarding the fluid properties is typically made beforehand. Firstly, the fluid is typically handled as incompressible - overlooking fluid density changes along the channel length. This is likely valid due to the low pressure drop of the monolith reactor. Some models also neglects changes in total molar flow rates - which should be fine for low reactant concentrations [26]. However, the most commonly used assumption, that comes with a plethora of implications and experimental requirements, is the single-channel assumption. It should be mentioned that there exist highly detailed **washcoat models** for flow inside porous networks [30]. Even though their results are interesting for development of e.g. pore diffusion models, their detailed descriptions are simply not viable on a monolith modelling level [26], and so they are outside the scope of this thesis.

2.4.1 Single channel assumption

The **single-channel models** assume that the reaction-diffusion process that occurs within the large number of channels in a monolith reactor can be represented by a single channel [22]. This implies that each channel inlet has identical temperature, volumetric flow rate as well as same gas composition - regardless of its radial position. This also assumes that the manufactured monolith has no substantial changes in washcoat properties in the radial direction (i.e. from channel to channel). These implications should be controlled and verified on a lab scale catalyst. However, there still exists a distribution of volumetric flow rates in the channels, resulting from the upstream parabolic velocity profile of the typically laminar flow. Nevertheless, this is simply how these models are developed [26]. The single-channel assumption, along with the design of an experimental rig, is investigated in publication I.

For full-scale applications, where these gradients are significant, **multi-channel models** account for flow maldistributions, radial heat losses etc. They commonly use results from single-channel models to performing weighting between a number of representative channels [22]. However, also these models are outside the scope of this project. The three different modelling levels, multi-channel (a), single-channel (b) and washcoat models (c), can be seen in figure 2.3.

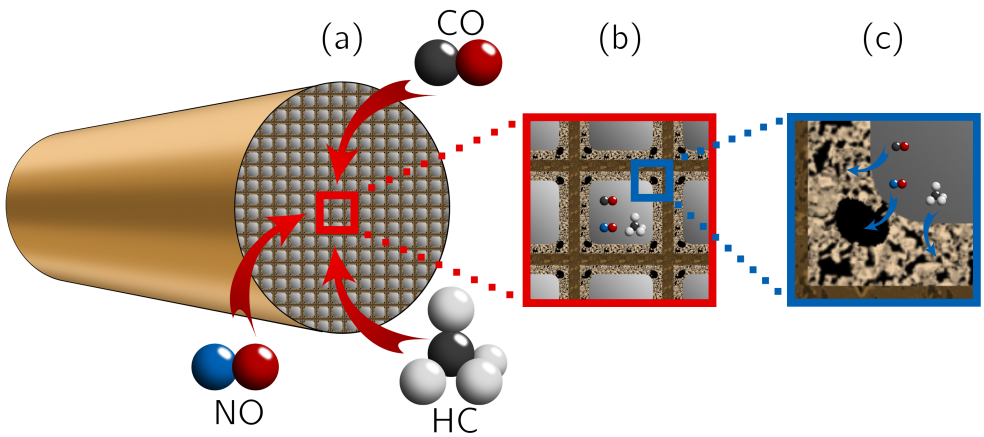

Figure 2.3: *Three common modelling levels of monolith reactor.*

2.5 Kinetics

There are different kinetic expressions with varying complexity and different physical meaning. The micro-kinetic models [31–34] usually include multiple elementary steps in a certain reaction while global models [35–38] describe the entire reaction with a single rate expression. The global models are generally predict reaction rates based on the gas phase concentrations while the micro-kinetic models include species adsorbed on the noble metal surface in the rate expressions. The elementary steps correspond to adsorption, dissociation, surface diffusion, surface reaction and desorption (see figure 2.1) - therefore the stoichoimetric coefficients for each step i equal to unity. The steps corresponds parts of a reaction that can be estimated through theory or experiments. The global kinetics describe the rate-determining step (usually the surface reaction step) and assume that the other steps are in equilibrium (e.g. adsorption and desorption). This reduces the necessary state variables for the rate expression, reducing computational demand and the stiffness (the equations are less sensitive to longer time steps) of the computation.

A typical rate expression is:

$$r = k_j c^{\nu} \tag{2.2}$$

where k_j $[1/s]$ is the rate constant, c $[mol/m^3]$ *or* $[-]$ is gas phase concentration or surface coverage and α $[-]$ is the soichiometric coefficient. The rate constant is calculated using the Arrhenius equation in centered form:

$$k_j = k0_j e^{-} \left(\frac{Ea_j}{R(T - T_{ref})} \right) \tag{2.3}$$

where $k0_j[m^3/s]$ is the rate constant at some reference temperature, T_{ref}:

$$k0_j = A_j e^{-} \left(\frac{Ea_j}{RT_{ref}} \right) \tag{2.4}$$

where A_j $[-]$ is the pre-exponential factor and Ea_j $[J/mol]$ is the activation energy. The centering of the Arrhenius equation reduces the otherwise strong correlation between the pre-expontial factor and the activation energy [39]. The reference temperature should be chosen so that it minimizes the correlation between A_j and Ea_j - although it is typically chosen as the average temperature of common operating temperatures.

2.6 Transport phenomenon

In order to predict the reaction rates along the channel, the mass transfer from the bulk gas to the solid surface (external) and throughout the washcoat (internal) must be taken into consideration. The same applies for heat transfer.

2.6.1 Tanks-in-series principle

The monolith channel can be treated as a plug flow reactor (PFR) which is modelled using the tanks-in-series model [40]. This non-ideal reactor model uses n continuously stirred tank reactors (CSTR) connected in series. As n assumes a larger number, the CSTRs behave increasingly like a PFR reactor as can be seen in figure 2.4.

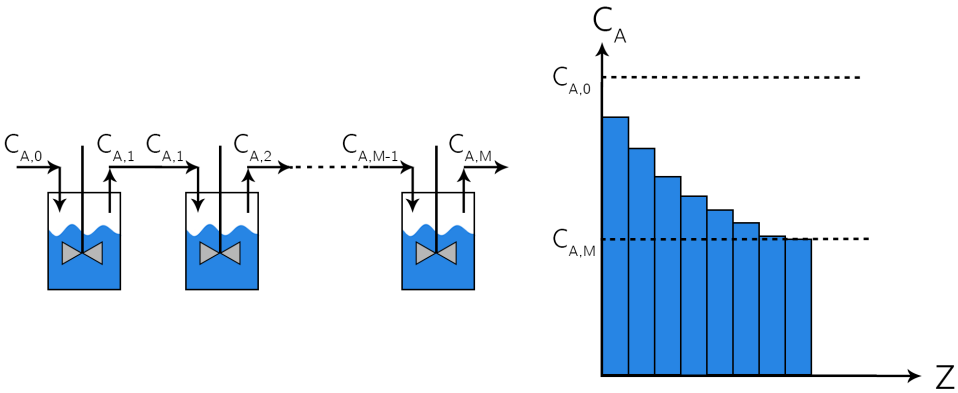

Figure 2.4: *Left: Tanks-in-series principle. Right: A typical graph for concentration vs axial reactor coordinate.*

2.6.2 External mass transfer

The flow inside the monolith channel is typically strictly laminar and for the greater part of the reactor treated as fully developed. The external mass transfer from the bulk gas to the solid surface is governed by molecular diffusion due to the concentration gradient that arises from the reaction within the washcoat. As such, the flux from the bulk gas to the solid interface is usually treated using film theory where the mass transfer coefficient is expressed in terms of the dimensionless Sherwood number [26]. Since the entrance length, where the laminar velocity profile develops, is very short compared to the length of the entire channel - the Sherwood number found in literature is typically given as an asymptotic value:

$$Sh_\infty = \frac{kc\, d_H}{D_{AB}} \tag{2.5}$$

where $Sh_\infty[-]$ is the asymptotic Sherwood number (typically between 2 and 7 depending on channel geometry [41, 42]), $kc[m/s]$ is the external mass transfer coefficient, $d_H[m]$ is the hydraulic diameter (typically the open channel diameter) and $D_{AB}[m^2/s]$ is the free molecular diffusivity. To account for the increased external mass transfer in the entrance region (in the case of a fixed wall temperature), Tronconi et al [41] developed the following correlation:

$$Sh_z = Nu_{\infty,T} + 6.874(1000z^*)^{-0.488}exp(-57.2z^*) \tag{2.6}$$

where $Sh_z[-]$ is the axially resolved Sherwood number, $Nu_{\infty,T}[-]$ is the Nusselt number for the relevant geometry and z^* is the axial coordinate in dimensionless form.

2.6.3 Internal mass transfer

There are a number of ways to treat the internal mass transfer through the washcoat. Some authors simply neglect internal mass transfer due to sufficiently thin washcoats or by operating at sufficiently low temperatures where the reaction is kinetically controlled [43, 44]. When it comes to operation of the automotive converters, internal diffusion limitations are apparent in normal operating conditions even with very thin washcoats [45, 46] – hence it is very common to include a separate model for the internal mass transfer [28, 47–55]. The option would be to lump the mass transfer effects into the kinetic expression [41], however it is not likely that such a model will accurately predict performance for an equally wide range of operating conditions as the models that separately model mass transfer.

2.6.3.1 Pore models

To model internal mass transfer properly, an estimate of the effective diffusivity is needed [22]. This can either be measured as explained in chapter 3 or modelled with one of the many available pore models; Wheeler's model [56], the model of Evans et al [57], the cylindrical model of Johnson and Stewart [58] to name a few. Each author has their own idea of how the pore network is arranged - e.g. as a tree where the smaller pores are branched from larger ones or arranged in series. The pore models often describe the diffusion in macro- and micro-pores, as a combination of free molecular diffusivity and Knudsen diffusivity, to form the pore diffusivity [59]. The Knudsen diffusivity, D_{Kn}, is the diffusion mechanism when the mean free path of the molecule ($\lambda \approx 140\ nm$ for O_2 at $1\ atm$ and $300\ ^\circ C$) is longer than the average micro pore diameter ($d_\mu \approx 5 - 10\ nm$):

$$D_{Kn} = \frac{d_\mu}{3}\sqrt{\frac{8RT}{\pi M}} \tag{2.7}$$

where $d_\mu\ [m]$ is the the average micro pore diameter, $R\ [m^3PaK^1mol^{-1}]$ is the gas constant, $T\ [K]$ is temperature and $M\ [g/mol]$ is the molecular mass. The free molecular diffusivity, D_{AB} is the diffusion mechanism when the mean free path of the molecule is shorter than the average macro pore diameter ($d_M \approx 1 - 10\ \mu m$). The free molecular diffusivity can be measured experimentally or calculated through the Chapman-Enskog method [60]:

$$D_{AB} = \frac{3}{16}\frac{(4\pi k_B T/M_{AB})^{1/2}}{n\pi\sigma_{AB}^2\Omega_D} \tag{2.8}$$

where $k_B\ [J/K]$ is Boltzmann's constant, $M_{AB}\ [g/mol]$ is the reduced molecular mass, $n\ [mol/m^3]$ is the number density of molecules in the mixture, $\sigma_{AB}^2\ [m]$ is the average

collision diameter and Ω_D $[-]$ is the collision integral. Which of these diffusion mechanisms that is the dominating one depends on the porous media and its pore size distribution. However, it is common to include both of these mechanisms to arrive at the arrive at the pore diffusivity, D_P, using the Bosanquet equation [59]:

$$D_P = \left(\frac{1}{D_{AB}} + \frac{1}{D_{Kn}} \right)^{-1} \tag{2.9}$$

To further describe the complex nature of the pore network, two common constants are used - tortuosity ($\tau \approx 1 - 10$) and porosity ($\epsilon \approx 0.8$). Figure 2.5 illustrates physical interpretations of these pore model constants.

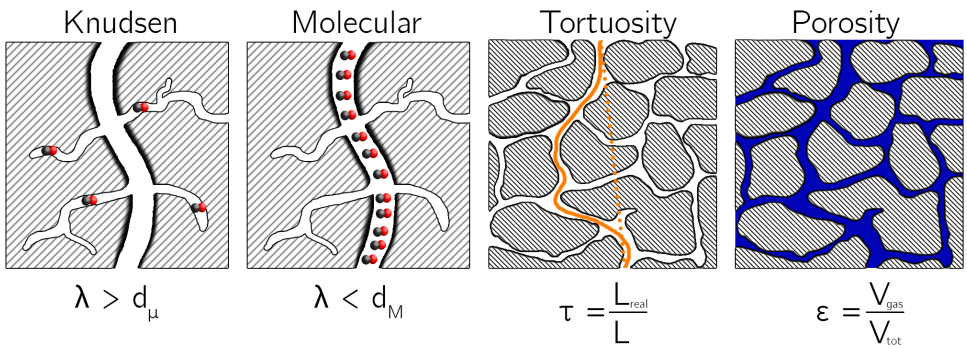

Figure 2.5: *Physical interpretations of pore model constants.*

The tortuosity is generally found to be inversely proportional to the washcoat porosity [61]. The porosity scales the pore diffusivity with the void fraction of the material while the tortuosity takes the curvature of the pores into account. In this thesis, Wheeler's pore model [56] is used:

$$Deff_i = \frac{\epsilon D_P}{\tau} \tag{2.10}$$

2.6.4 Discretization schemes of single-channel models

The two most common ways to include internal mass transfer limitations in automotive converters are 1D models with the use of an effectiveness factor [47–51] as well as the 1+1D models [28, 52–55]. On a general level, these methods are distinguished by the fact that the 1+1D model also resolve the washcoat in the radial direction. Thus each tank, in the tanks-in-series model, includes a set of sub-tanks which correspond to washcoat layers [52].

2.6.4.1 1D models with effectiveness factor

The 1D reactor model, using an effectiveness factor, is far less complex than the 1+1D models. As a consequence it is less stiff and faster to compute [26]. The effectiveness factor is a simple but powerful tool that can account for different washcoat formulations, washcoat geometries, states of aging etc - but needs to be tuned or calculated for every state of the material and inlet conditions [62]. Because it is so inexpensive, it is commonly used for commercial operation or control purposes [62]. Apart from simple tuning the constant to fit kinetic data there exist analytical solutions [63] as well as numerical solutions [48, 62, 64] to the problem.

2.6.4.2 1+1D models

For improved accuracy and understanding - which is key for reactor design and optimization, the 1+1D model is a much better choice [47]. The name implies that the gas phase is resolved axially while the washcoat is resolved in radial direction as well ("+1D") as seen in figure 2.6. However, it is not two dimensional by definition, since the axial mass transfer within the washcoat is usually negligated. All of these models rely on the washcoat being axisymmetric, thus the tangential dimension is removed. However, this assumption has been reported to be quite erronous and its penalties could unfortunately result in inaccurate light-off temperature predictions [65]. This assumption is elaborated on in publication III, where an alternative to the classical 1+1D model is presented - through which the axis-symmetric requirement can be circumvented.

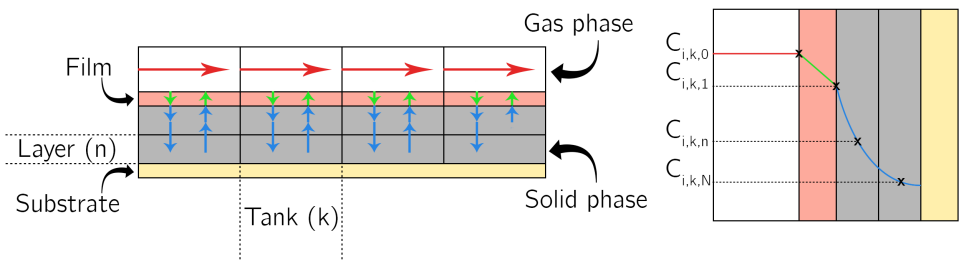

Figure 2.6: *Left: Tanks-in-series principle applied for a 1+1D discretization scheme. Right: Concentration profile.*

Lastly, there exist some attempts at performing full 3D CFD simulations of a single-channel [65]. As mentioned, they demonstrate some valuable insights for the validity of the underlying assumptions for the 1+1D models. However, these models are significantly more computationally demanding than the more common 1D and 1+1D models.

2.6.5 Heat transfer

Heat transfer in the monolith is to some extent analogous to the external mass transfer, i.e. a Nusselt correlation is used to describe the heat transfer from the gas phase to the solid [41]:

$$Nu_{\infty} = \frac{h\, d_H}{k} \tag{2.11}$$

where $Nu_{\infty}[-]$ is the asymptotic Nusselt number (typically between 3.0 and 4.5 [66]), $h\ [W/(m^2\, K)]$ is the heat transfer coefficient, $d_H\ [m]$ is the hydraulic diameter (typically the open channel diameter) and $k\ [W/(m\, K)]$ is the gas phase conductivity. Other important heat transport mechanisms include conduction within the washcoat and monolith substrates (especially important for metallic substrates) and reaction heat since the majority of the catalytic reactions in the EATS are exothermic. In this thesis, there is little or no focus on heat transfer since the experiments performed on lab-scale are more or less isothermal due to the low reactant concentration and high volumetric flow rates. However, in a multi-channel model, where temperature gradients are significant, heat losses have to be modelled.

3 Modelling and Experiments

This chapter describes the 1+1D model in more detail along with the performed experiments. For additional information, please refer to publication III and the works by Lundberg et al [52, 53].

3.1 Original 1+1D model

The 1+1D reactor model is based on the ones developed by Lundberg et al [52, 53] and in turn the one by Ericsson et al [67]. This model is a good trade-off between computational speed (running in real-time on a i7-4600 U, 2,7 GHz processor) and accuracy [47].

3.1.1 Mass transfer

The model contains a quasi-steady state (assuming that the variations in inlet conditions are slow in comparison with the timescales for the modelled chemical processes) formulation of mass and heat balances. From hereafter, the discretized nodes in the tanks-in-series model are distinguished between axial nodes, referred to as *tanks* (index k), and radial nodes, referred to as *layers* (index n). Substances are indexed by i and reactions by j. The mass balance for the gas phase ($n = 0$) is given by:

$$0 = \left(V_{k,0} \frac{dc_{i,k,0}}{dt} \right) = F_{tot} \left(y_{i,[k-1],0} - y_{i,k,0} \right) - \Gamma_{i,k,0} \left(c_{i,k,0} - c_{i,k,1} \right) \tag{3.1}$$

The terms (from left to right) correspond to changes in the amount of substance in tanks corresponding to the gas phase, advection by bulk flow and lastly external mass transfer. For all layers ($n > 0$) the washcoat mass balance is given by:

$$\begin{aligned} 0 = \left(V_{k,n} \epsilon \frac{dc_{i,k,n}}{dt} \right) = \Gamma_{i,k,[n-1]} \left(c_{i,k,[n-1]} - c_{i,k,n} \right) - \\ - \Gamma_{i,k,n} \left(c_{i,k,n} - c_{i,k,[n+1]} \right) + \sum_j v_{i,j} r_{j,k,n} m_{k,n} \end{aligned} \tag{3.2}$$

Here, the mass transfer terms correspond to internal mass transfer and the last term is a source term, corresponding to production or consumption via reaction. The external mass transfer coefficient, $\Gamma_{i,k,0}$, and the internal mass transfer coefficient, $\Gamma_{i,k,n}$ is calculated as:

$$\Gamma_{i,k,0} = \frac{A_k}{\frac{1}{kc_{i,k,0}} + \frac{0.5\Delta x_1}{Deff_{i,k,n}}} \tag{3.3}$$

$$\Gamma_{i,k,n} = \frac{Deff_{i,j,n} A_k}{0.5\Delta x_n + 0.5\Delta x_{[n+1]}} \tag{3.4}$$

For the last layer ($n = N$), it is assumed that there is no flux into the monolith substrate, i.e. $\Gamma_{i,k,N} = 0$. Due to very low reactant concentration along with high space velocities, it is likely that the operation of the lab-scale monolith is isothermal. Hence, the models for heat transfer is not further presented. For details, see [53].

3.1.2 Kinetics

The detailed kinetics model used includes oxidation of CO, NO and hydrocarbons lumped as HC. However, as the oxidation of NO on Pt has significantly higher activiation energy than CO and HC, it is very hard to achieve a differential reactor for all these reactants at the same time. As a result, the project has focused on NO oxidation up to this point. The detailed reaction scheme for HC and CO oxidation can be found in [53]. The NO oxidation reaction scheme, based on Lundberg et al and Olsson et al [52, 68], includes adsorption and desorption for O_2 and NO_2 as well as backwards and forwards surface reaction as can bee seen in table 3.1.

Table 3.1: Detailed reaction scheme for NO oxidation.

#	Mechanism	Reaction	Rate
1	O_2 adsorption	$O_2(g) + 2* \rightarrow 2O^*$	$r_1 = k_1 C_{O_2} \theta_V^2$
2	O_2 desorption	$2O^* \rightarrow O_2(g) + 2*$	$r_2 = k_2 \theta_O^2$
3	NO_2 adsorption	$NO_2(g) + 1* \rightarrow NO_2^*$	$r_3 = k_3 C_{NO_2} \theta_V$
4	NO_2 desorption	$NO_2^* \rightarrow NO_2(g) + 1*$	$r_4 = k_4 \theta_{NO_2}$
5	surface reaction	$NO(g) + O^* \rightarrow NO_2^*$	$r_5 = k_5 C_{NO} \theta_O$
6	surface reaction	$NO_2^* \rightarrow NO(g) + O^*$	$r_6 = k_6 \theta_{NO_2}$

3.2 Parallel 1+1D model

To be able to handle arbitrary washcoat geometries with local features such as cracks, thus circumventing the assumption of an axissymmetric assumption, a sectionalizing principle was applied to the 1+1D model. Similarly to Papadias et al [51, 62] and later Hayes et al [49], the washcoat is sectionalized into multiple slices as seen in figure 3.1. Whereas Papadias et al and Hayes et al used this principle to calculate an overall effectiveness factor, in publication III this method is used to account for the importance of local or global washcoat properties (porosity, tortuosity and thickness). It is assumed that potential tangential mass transfer is negligible compared to the radial one. The local washcoat properties are determined using a combination of scanning electron microscopy (SEM) analysis and gravimetric analysis (GA). Once these properties are established the model treats the problem, of a non-uniform washcoat, as a number of parallel computations using the original 1+1D model.

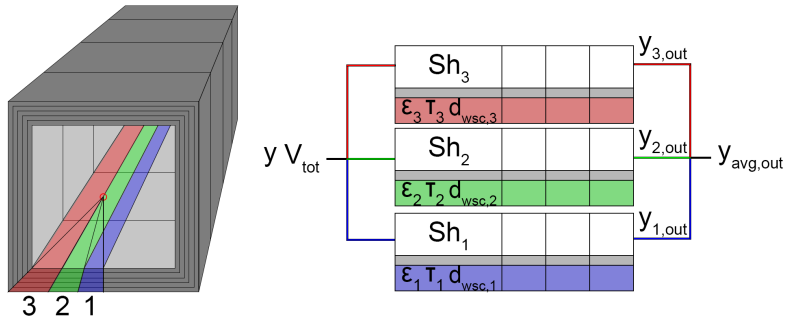

Figure 3.1: *Parallel 1+1D model discretization scheme and parallel computing scheme.*

3.3 Design of Experiments

In order to able to model monolith reactors properly experimental observations are required. To systematically examine these observations, and to get the most data out of the least number of experiments, design of experiment (DoE) is an invaluable tool. DoE aids in determining the relationship between state variables and some observed process variable [69]. To be able to model the processes that could occur in the monolith, the data that is used to tune the model must also contain them. In order to create a broad experimental space, the effect of the the following parameters, presented in table 3.2 are investigated.

Table 3.2: Investigated parameters for catalyst modelling.

Variable	Typical value
Temperature	100 to 500°C
Volumetric flow rate	20 to 40 l_N/min
	95′000 to 190′000 hr^{-1}
Reactants	CO, NO, C_3H_6
Inlet concentration	100 or 1000 ppm
Mass of active catalyst	5 or 15 g/ft^3
	0.29, 0.33 or 0.67 $\%w/w$
Thickness of washcoat	28, 55 or 110 μm

Furthermore, since the operation of automotive converters are highly transients, it is required that their mathematical models are the same. For such models, Berger et al [70] suggested that transient experiments are performed - simply because they contain much more information than the steady-state counterpart.

3.4 Synthetic Catalyst Activity Test

In engine tests, the exhaust data, e.g. temperature and concentration, is often highly correlated [71]. To be able to cover a large experimental space and to freely adjust parameters in experiments, it is therefore common to use a synthetic catalyst activity test (SCAT) bench - also commonly known as flow reactor. The SCAT system used in this project is carefully described and evaluated for use in transient experiments in publication I, hence only its main principle and features are emphasized here.

The SCAT bench uses separate sources for each desired reactant, where the inlet concentrations are controlled using mass flow controllers (MFC). N_2 is commonly used as a carrier gas and the entire mixture is heated using an electrical heater. In this way, any combination of reactant concentration, flow rate and temperature can be achieved. The diesel oxidation catalysts, typically 1x1 inch, are placed in a large oven which encases the entire reactor. The SCAT bench allows for measurement of temperature, pressure, concentration and flow rate at multiple given positions.

3.4.1 Kinetic experiments

The kinetic experiments, summarized in publication II, comprise concentration step experiments for several reasons. Firstly, again, the transient experiments contain more useful information. Secondly, the short duration of the steps (where reaction occurs) limits the likelihood of a change in the noble metal oxidation state - which can alter the kinetics significantly [1]. As of now, this phenomenon is not included in the 1+1D model, hence, to observe this is experimentally undesired. Lastly, the step changes can be seen to mimic what happens in an engine when the load points rapidly change.

3.4.2 Temperature programmed desorption

As was discussed in the introduction, the most important parameter for reaction (besides the temperature) is the available surface area of the catalyst. This can be determined using temperature programmed desorption (TPD) [72]. In this experimental procedure seen in figure 3.2, the reactor temperature is set very low to allow for adsorption but not reaction. A well-known concentration of e.g. CO is dosed in two separate pulses. The first pulse (blue curve) shows uptake of CO until the 100 second mark. At this point the active sites are saturated and therefore CO starts to "leak" through the catalyst. This uptake of CO includes physisorption and chemisorption. After the MFC is switched off, the physisorbed molecules desorb. A second pulse is performed and the second uptake corresponds to physisorption (since the chemisorbed sites are already saturated). The difference between uptake one and two corresponds to the amount of chemisorbed molecules which is a direct measurement of how many active sites the catalyst contains.

By dividing with the total amount of catalyst (in substance amount) the so-called dispersion is achieved. This measurement (usually below 30% of the total catalyst amount) describes the accessibility of the precious metal, or in words a qualitative measurement of

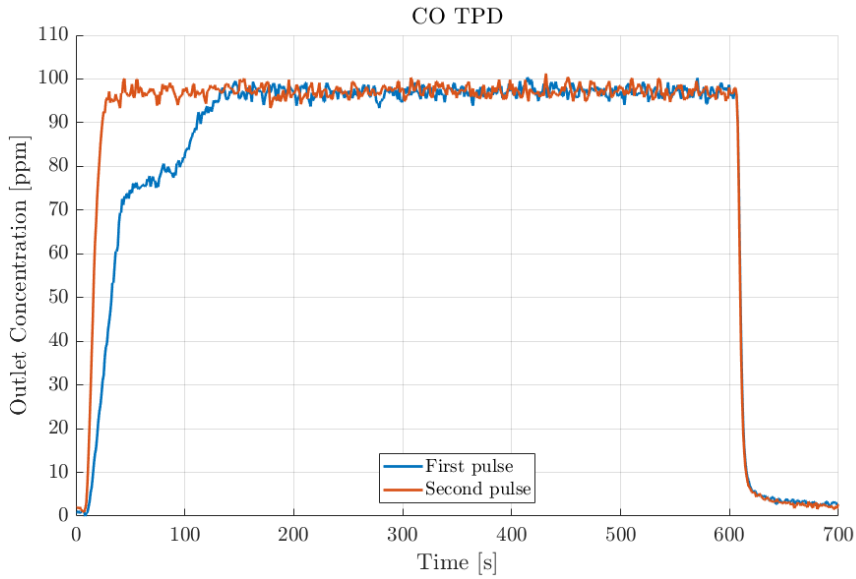

Figure 3.2: *CO TPD principle.*

the efficiency of the washcoat and catalyst preparation. As this parameter linearly scales the reaction rates, expressed as moles/s/kg of catalyst, this input is of utmost importance for modelling.

3.5 Scanning Electron Microscope imaging

The scanning electron microscope (SEM) resembles the modern digital camera. However, instead of detecting the light reflected by an object, an accelerated electron (primary electrons) beam is bombarded onto a surface of interest. This surface allows for some electrons to pass through (transmitted electrons) - however, during this process, the surface itself produces reflected electrons (secondary or backscattered electrons). The intensity of these secondary electrons can be recorded using special solid-state detectors and amplified to form a pixel luminosity. The electron beam is then moved (scanned) into a new position to record a new pixel - and slowly an image is captured [73]. A typical image of the monolith substrate (upper left), the open channel (lower right) and the applied washcoat can be seen in figure 3.3.

In this project, as explained further in publication III, SEM images are used to measure the washcoat thickness using cross-sectional images of the monolith channel. The open source plugin ImageJ was also used, in combination with a threshold script, to differentiate between gas and solid phase - enabling approximations of local porosity. These two values form the basis for tuning a tangentially resolved effective diffusivity.

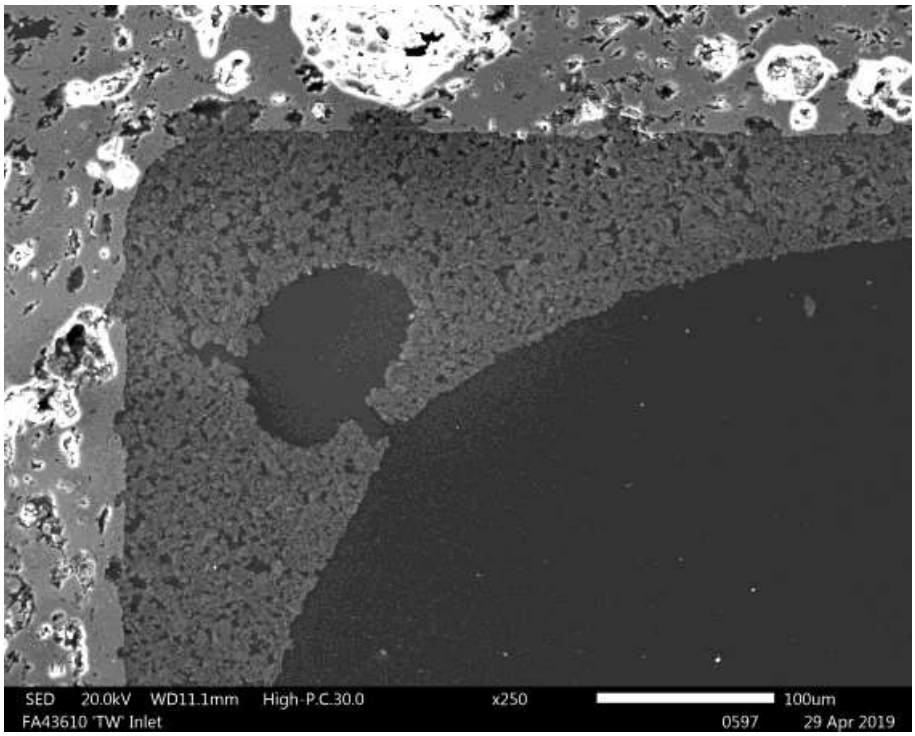

Figure 3.3: *SEM image of open monolith channel and washcoat.*

3.6 Gravimetric Analysis

There are several methods for measuring effective diffusivity for washcoats applied onto monolith substrates [59, 74, 75]. Hayes et al [59] constructed a modified Wicke-Kallenbach cell to measure the diffusivity between channels for a washcoated monolith reactor. By also measuring the diffusive resistance of the uncoated monolith - the diffusivity of the coating alone can be distinguished. There are also classical chromatographic methods which rely on long columns ($>> 1\,m$) containing crushed monoliths with applied washcoat [74]. The chromatographic methods rely on small differences in residence time, across these columns, as a result from the effective diffusivity of some tracer substance. Lastly, there are gravimetric methods [75]. These are tedious experiments and only result in single data points per several of hours of experiments - however, they are accurate since they directly measure the uptake of some reactant with time.

In gravimetric analysis (GA) a small sample of washcoated monolith is placed on a balance inside a thermally insulated chamber. The chamber is heated, and simultaneously evacuated, to desorb any previously adsorbed molecules - to start with a fresh sample. The chamber is then cooled to a low temperature (usually around $0°C$) where the molecular diffusivity is greatly reduced. The previously evacuated chamber is then exposed to a large slowly diffusing hydrocarbon, e.g. hexane, which is kept in a separate liquid reservoir. The

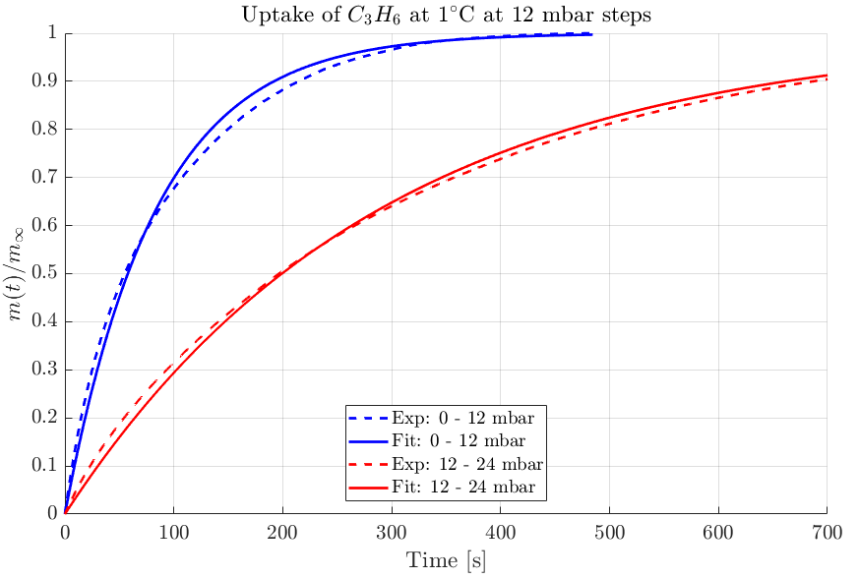

Figure 3.4: *Uptake of C_3H_6 at 1°C at 12 mbar steps.*

hydrocarbon adsorbs onto the washcoated sample and its uptake is monitored over time. From these uptake curves, seen in figure 3.4 the effective diffusivity can be calculated from curve fitting:

$$\frac{m(t)}{m_\infty} = 1 - e^{-kt} \tag{3.5}$$

where $m(t)/m_\infty$ $[-]$ is the ratio of mass adsorbed at time t $[s]$ to mass adsorbed at equilibrium. k $[s^{-1}]$ is the uptake rate coefficient:

$$k = \frac{Deff}{d_{wsc}^2} \tag{3.6}$$

where $Deff$ $[m^2]$ is the effective diffusivity and d_{wsc} $[m]$ is the effective diffusion length - i.e. the washcoat thickness. Using the previously mentioned pore diffusion models, the tortuosity constant can be estimated. Once the effective diffusivity, washcoat porosity and thickness has been established through SEM and IGA, we can study the effects of mass transfer resistance. By separately measuring the mass transfer properties of the washcoat, there is less need for tuning when performing parameter estimation - or at least the results from IGA and SEM should provide a good starting point for tuning.

4 Results and Discussion

This chapter summarizes the results from publications I, II and III.

4.1 Summary of publication I - Use of 3D-printed mixers in laboratory reactor design for modelling of heterogeneous catalytic converters

Publication I presents a through investigation of the benefits and drawbacks of two typical SCAT bench designs - the premixed and injection-based design. The premixed design mixes the reactant flow before heating it to the desired operating temperature. As a result the premixed design unfortunately has high axial dispersion which is not desired in highly transient experiments. The injection-based design circumvents the problem with axial dispersion through injection of the reactants through a set of capillaries close to the reactor inlet. Because of this design principle, there is a risk of having a maldistribution of reactants across the monolith inlet - which is not accounted for in the single-channel models. The problem is that very few SCAT benches allow you to measure this local problem since you only have access to mixed-cup averages of the outlet conditions.

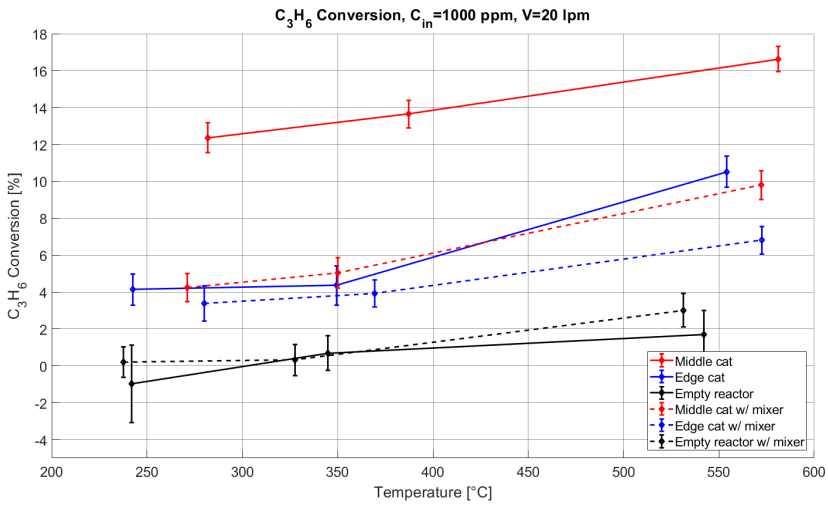

Figure 4.1: *Conversion vs temperature for various catalyst configurations, with or without mixer.*

To tackle this problem a set of smart catalysts were designed. The catalysts only induce local reactions and so the reactivity (and thus inlet concentrations) can be measured at various radial positions. The results can be seen in figure 4.1. By comparing the blue and red solid lines, it can be seen that the conversion depends on the radial position. To solve

this maldistribution problem a modified SMX mixer was designed. Once the experiments were repeated using the mixer upstream the catalyst sample (dotted lines), conversions did not show a radial dependence. The SCAT bench, along with the modified SMX mixer, was also simulated using computational fluid dynamics (CFD). The effect on the flow field, caused by the mixer can be seen in figure 4.2.

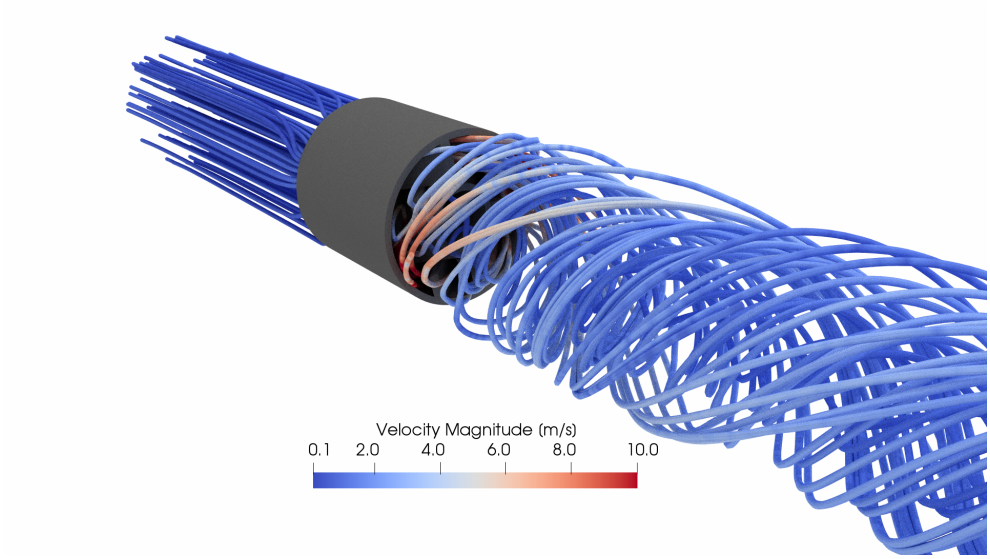

Figure 4.2: *Streamlines colored by velocity magnitude for CFD simulation of 20 LN/min.*

4.2 Summary of publication II - Efficient Experimental Approach to Evaluate Mass Trans-fer Limitations for Monolithic DOCs

In publication II, the diesel oxidation catalyst (DOC, Pt/-Al2O3) is used in a synthetic-gas catalyst test bench to study internal and external mass transfer limitations during NO oxidation. By varying the washcoat thickness (55 and 110μm) while keeping the total noble metal loading the same, two DOCs can be evaluated using classical timescales. Figure 4.3 shows the ratio between the time constant for reaction and washcoat diffusion. The conversion for the DOC with thinner washcoat shows to be kinetically controlled at lower temperatures. At intermediate temperatures it enters a region where internal mass transfer limitations start to play a role. The conversion for the DOC with thicker washcoat shows severe internal mass transfer limitations already at around 175°C.

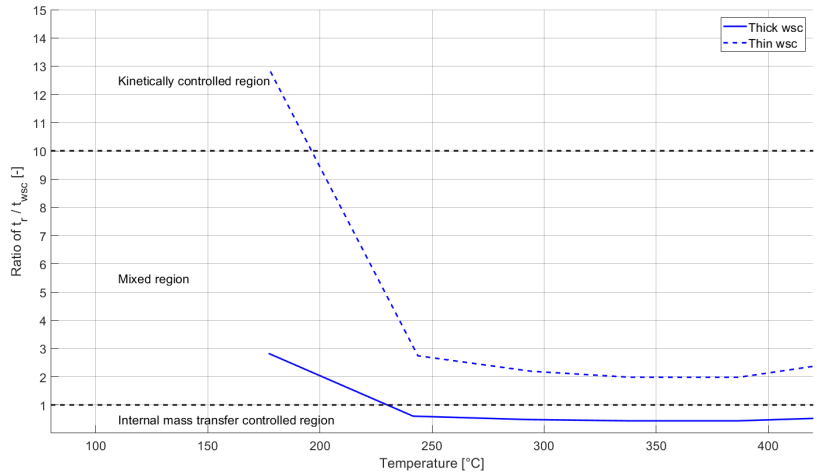

Figure 4.3: *Ratio of time scale for reaction and washcoat diffusion.*

4.3 Summary of publication III - Modelling of mass-transfer resistances in non-uniformly washcoated monolith reactors

The traditional 1D or 1+1D single-channel models fail to capture variations in mass transfer resulting from a non-uniform washcoat. Publication III presents a modelling framework where a sectionalizing principle is combined with a traditional 1+1D model to account for local variations in the washcoat. Intelligent gravimetric analysis (IGA) and scanning electron microscopy (SEM) are used in combination to calculate local effective diffusivity as an input for each simulation. The new model is compared to the original 1+1D model in figure 4.4, where NO light-off curves are shown. The new model predicted increased conversion at elevated temperatures, where mass transfer limitations are present, due to the higher porosity in the corners. Hence, these local features are important for predictive modelling of automotive converters where the axis-symmetric assumption for washcoat thickness is not fulfilled.

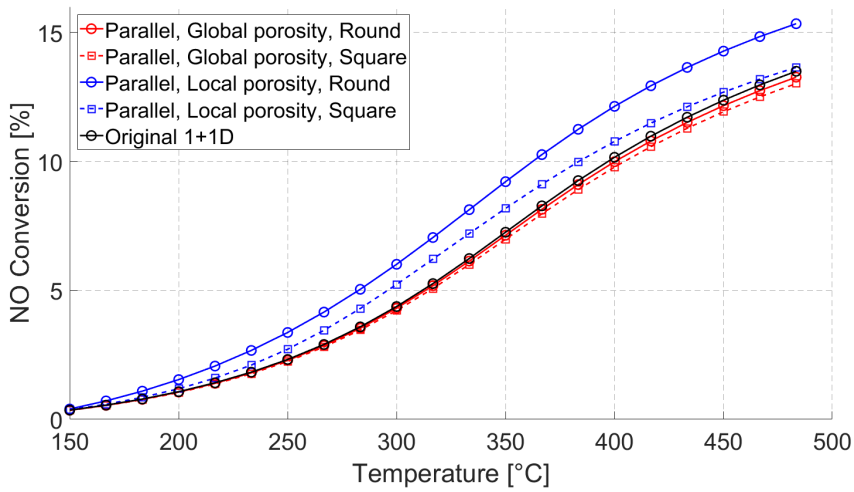

Figure 4.4: *Light-off curves for the original 1+1D model new (parallel) model using either global or local washcoat features*

.

5 Conclusion and Outlook

From publication II and III it is evident that internal mass transfer play an important role in NO oxidation, even at very low temperatures, and that it must be modelled with great care. It is also clear that neither experiments, nor simulations, can independently enhance understanding of e.g. the corner effects of the washcoat. That is, it is virtually impossible to design experiments that can determine how the washcoat corners affect the mass transfer. Likewise, modelling alone would not have been able to even identify the fact that the washcoat accumulates in the corners of the channel. Furthermore, this thesis highlights the importance of investigating experimental boundary conditions and model simplifications - whose validity otherwise would have been taken for granted.

As of now, the parallel model shows promising results. That is, it shows some sensitivity compared to the original model. Still, that does not mean that it can separate mass transfer and kinetic effects better than the 1+1D model. For that to be investigated the parallel model has to be tuned separately from the original model. The tuned parameters, e.g. activation energy, can then be compared to literature data to evaluate which model is actually more accurate. The additional computation cost also has to be considered. Is having to run multiple simulations really worth the potential increase in accuracy for the parallel model - even if they computed in parallel? For development of future automotive converters it might be useful if future coating techniques do not change the washcoat distribution, but for real-time monitoring and EATS control on board an electronic control unit (ECU) it is far too computationally demanding.

The next investigation will be to use oxidation catalysts with an inert layer of washcoat on top of the catalytically active washcoat layer. This allows for mass transfer resistances to be emphasized further, even for very fast oxidation reactions - such as CO and HC oxidation. Moreover, it could be interesting to use more realistic inlet compositions to mimic common exhaust gas, e.g. inclusion of water and various hydrocarbons. At a later stage, the single channel models will be applied to a full-scale catalyst used in an engine test bench. At that point it would be interesting to compare the single-channel model with a multi-channel model using CFD to include distributions of flow rate and temperature.

6 Contribution to the field

This main contribution of this work can be summarized as:

6.1 Publication I

"Use of 3D-printed mixers in laboratory reactor design for modelling of heterogeneous catalytic converters"

Validation of boundary conditions is of utmost importance - no matter the discipline. The novelty in this work comes from the smart way of identifying radial concentration maldistributions where local measurements are not possible. The modified SMX mixer assembled through additive manufacturing in $\alpha - Al_2O_3$, having the reactant injection point in the turbulent wake of the mixer, is also new. I was responsible for designing the experiment, catalysts and the mixer - as well as writing the paper, analyzing the kinetic data and performing the dispersion calculations.

6.2 Publication II

"Efficient Experimental Approach to Evaluate Mass Trans-fer Limitations for Monolithic DOCs"

Experimental screening and its associated analysis, is of importance for time efficient experimental campaigns. These types of screenings have been done by others, however, the novelty here comes from using a sufficiently thin washcoat for one of the experiments - so that its reaction time scales can be carried over to the DOC with thick washcoat. Otherwise some modelling of reaction time scales would have been required. I was responsible for design of experiments, analysis as well as writing the paper.

6.3 Publication III

"Modelling of mass-transfer resistances in non-uniformlywashcoated monolith reactors"

The often disregarded and erroneous assumption, regarding an axissymetric washcoat formulation, is typically found in all papers for 2D single-channel models. The novelty here comes from trying to circumvent this problem by resorting to the sectionalizing principle. Also, the combined use of IGA and SEM to tune a local effective diffusivity is also new. I was responsible for developing the idea, perfoming IGA experiments and analysis of SEM images, the modelling itself and lastly writing the paper.

Bibliography

[1] April Russell and William S. Epling. "Diesel Oxidation Catalysts". In: *Catalysis Reviews* 53.4 (2011), pp. 337–423. ISSN: 0161-4940. DOI: 10.1080/01614940.2011.596429. URL: https://doi.org/10.1080/01614940.2011.596429.

[2] European Environmental Agency (EEA). *Sulphur dioxide (SO2) emissions*. 2015. URL: https://www.eea.europa.eu/data-and-maps/indicators/eea-32-sulphur-dioxide-so2-emissions-1/assessment-3 (visited on 01/07/2020).

[3] Louise W. Kao and Kristine A. Nañagas. "Toxicity Associated with Carbon Monoxide". In: *Clinics in Laboratory Medicine* 26.1 (2006). Clinical Toxicology, pp. 99 –125. ISSN: 0272-2712. DOI: https://doi.org/10.1016/j.cll.2006.01.005. URL: http://www.sciencedirect.com/science/article/pii/S0272271206000060.

[4] Organization World Health. *Ambient air pollution: a global assessment of exposure and burden of disease*. Geneva: World Health Organization, 2016. ISBN: 9789241511353. URL: https://apps.who.int/iris/handle/10665/250141.

[5] Theo M.C.M. de Kok, Hermen A.L. Driece, Janneke G.F. Hogervorst, and Jacob J. Briedé. "Toxicological assessment of ambient and traffic-related particulate matter: A review of recent studies". In: *Mutation Research/Reviews in Mutation Research* 613.2 (2006), pp. 103 –122. ISSN: 1383-5742. DOI: https://doi.org/10.1016/j.mrrev.2006.07.001. URL: http://www.sciencedirect.com/science/article/pii/S1383574206000433.

[6] Roger O. McClellan, Thomas W. Hesterberg, and John C. Wall. "Evaluation of carcinogenic hazard of diesel engine exhaust needs to consider revolutionary changes in diesel technology". In: *Regulatory Toxicology and Pharmacology* 63.2 (2012), pp. 225 –258. ISSN: 0273-2300. DOI: https://doi.org/10.1016/j.yrtph.2012.04.005. URL: http://www.sciencedirect.com/science/article/pii/S0273230012000694.

[7] Martyn V. Twigg. "Rôles of catalytic oxidation in control of vehicle exhaust emissions". In: *Catalysis Today* 117.4 (2006). Selected papers presented at the 6th International Workshop on Catalytic Combustion, pp. 407 –418. ISSN: 0920-5861. DOI: https://doi.org/10.1016/j.cattod.2006.06.044. URL: http://www.sciencedirect.com/science/article/pii/S0920586106004196.

[8] V.I. Pârvulescu, P. Grange, and B. Delmon. "Catalytic removal of NO". In: *Catalysis Today* 46.4 (1998), pp. 233 –316. ISSN: 0920-5861. DOI: https://doi.org/10.1016/S0920-5861(98)00399-X. URL: http://www.sciencedirect.com/science/article/pii/S092058619800399X.

[9] P. G. Rogers. “The Clean Air Act of 1970”. In: *EPA Journal* 16.1 (1970), pp. 21 –23. URL: https://www.epa.gov/history/epa-history-clean-air-act-19701977.

[10] “COUNCIL DIRECTIVE of 20 March 1970 on the approximation of the laws of the Member States relating to measures to be taken against air pollution by gases from positive-ignition engines of motor vehicles”. In: *Official Journal of the European Union* 1 (1970), pp. 171 –191. URL: https://eur-lex.europa.eu/legal-content/EN/ALL/?uri=CELEX:31970L0220.

[11] S. C. Davis and R. G. Boundy. *Transportation Energy Data Book*. English. Oak Ridge National Laboratory, Aug. 2019.

[12] M. V Twigg and Imperial Chemical Industries PLC. Agricultural Division. Catalyst handbook. *Catalyst handbook*. 2nd ed. London : Manson Pub, 1996. ISBN: 1874545359. URL: http://www.loc.gov/catdir/enhancements/fy0638/97216179-t.html.

[13] Masaoki Iwasaki and Hirofumi Shinjoh. “A comparative study of “standard”, “fast” and “NO2” SCR reactions over Fe/zeolite catalyst”. In: *Applied Catalysis A: General* 390.1 (2010), pp. 71 –77. ISSN: 0926-860X. DOI: https://doi.org/10.1016/j.apcata.2010.09.034. URL: http://www.sciencedirect.com/science/article/pii/S0926860X10006885.

[14] Kanta Yamamoto, Keishi Takada, Jin Kusaka, Yasuharu Kanno, and Makoto Nagata. “Influence of Diesel Post Injection Timing on HC Emissions and Catalytic Oxidation Performance”. In: *Powertrain Fluid Systems Conference and Exhibition*. SAE International, 2006. DOI: https://doi.org/10.4271/2006-01-3442. URL: https://doi.org/10.4271/2006-01-3442.

[15] P. Ehrburger, J.-F. Brilhac, Y. Drouillot, V. Logie, and P. Gilot. “Reactivity of Soot With Nitrogen Oxides in Exhaust Stream”. In: *Spring Fuels Lubricants Meeting Exhibition*. SAE International, 2002. DOI: https://doi.org/10.4271/2002-01-1683. URL: https://doi.org/10.4271/2002-01-1683.

[16] Sung Dae Yim, Soo Jean Kim, Joon Hyun Baik, InSik Nam, Young Sun Mok, Jong-Hwan Lee, Byong K. Cho, and Se H. Oh. “Decomposition of Urea into NH3 for the SCR Process”. In: *Industrial & Engineering Chemistry Research* 43.16 (2004), pp. 4856–4863. DOI: 10.1021/ie034052j. URL: https://doi.org/10.1021/ie034052j.

[17] Massimo Colombo, Isabella Nova, Enrico Tronconi, Volker Schmeißer, Brigitte Bandl-Konrad, and Lisa Zimmermann. “Experimental and modeling study of a dual-layer (SCR+PGM) NH3 slip monolith catalyst (ASC) for automotive SCR aftertreatment systems. Part 1. Kinetics for the PGM component and analysis of SCR/PGM interactions”. In: *Applied Catalysis B: Environmental* 142-143 (2013), pp. 861 –876. ISSN: 0926-3373. DOI: https://doi.org/10.1016/j.apcatb.2012.10.031. URL: http://www.sciencedirect.com/science/article/pii/S0926337312005103.

[18] J. J. Berzelius. *Årsberättelse om framstegen i Fysik och Kemi*. P. A. Norstedt Söner, 1835. URL: https://books.google.se/books/about/\%C3\%85rsber\%C3\%A4ttelse_om_framstegen_i_fysik_oc.html?id=1DM1AAAAcAAJ&redir_esc=y.

[19] A. J. B. Robertson. "The Early History of Catalysis". In: *Platinum Metals Review* 19 (2 1975), pp. 64 –69. URL: https://www.technology.matthey.com/article/19/2/64-69/.

[20] "VIII. Some new experiments and observations on the combustion of gaseous mixtures, with an account of a method of preserving a continued light in mixtures of inflammable gases and air without flame". In: *Philosophical Transactions of the Royal Society of London* 107 (Jan. 1817), pp. 77–85. DOI: 10.1098/rstl.1817.0009. URL: https://doi.org/10.1098/rstl.1817.0009.

[21] I. Chorkendorff. *Concepts of Modern Catalysis and Kinetics*. Wiley-VCH, 2003. ISBN: 3527305742. URL: https://www.xarg.org/ref/a/3527305742/.

[22] Zeynep Ilsen Önsan and Ahmet Kerim Avci. "Monolith reactors". In: *Multiphase Catalytic Reactors - Theory, Design, Manufacturing, and Applications*. John Wiley Sons, 2016. ISBN: 978-1-118-11576-3. URL: https://app.knovel.com/hotlink/pdf/id:kt011BVFG1/multiphase-catalytic/performance-evaluation.

[23] Xiaobo Song, Jeffrey D Naber, and John H Johnson. "A study of the effects of NH3 maldistribution on a urea-selective catalytic reduction system". In: *International Journal of Engine Research* 16.2 (2015), pp. 213–222. DOI: 10.1177/1468087414532462. URL: https://doi.org/10.1177/1468087414532462.

[24] Leonardo Giani, Gianpiero Groppi, and Enrico Tronconi. "Mass-Transfer Characterization of Metallic Foams as Supports for Structured Catalysts". In: *Industrial & Engineering Chemistry Research* 44.14 (2005), pp. 4993–5002. DOI: 10.1021/ie0490886. URL: https://doi.org/10.1021/ie0490886.

[25] Pranit S. Metkar, Vemuri Balakotaiah, and Michael P. Harold. "Experimental study of mass transfer limitations in Fe- and Cu-zeolite-based NH3-SCR monolithic catalysts". In: *Chemical Engineering Science* 66.21 (2011), pp. 5192–5203. ISSN: 00092509. DOI: 10.1016/j.ces.2011.07.014.

[26] Jinwen Chen, Hong Yang, Neil Wang, Zbigniew Ring, and Tadeusz Dabros. "Mathematical modeling of monolith catalysts and reactors for gas phase reactions". In: *Applied Catalysis A: General* 345.1 (2008), pp. 1–11. ISSN: 0926-860X. DOI: https://doi.org/10.1016/j.apcata.2008.04.010. URL: http://www.sciencedirect.com/science/article/pii/S0926860X08002251.

[27] Shaibal Roy, Tobias Bauer, Muthanna Al-Dahhan, Peter Lehner, and Thomas Turek. "Monoliths as multiphase reactors: A review". In: *AIChE Journal* 50 (2004), pp. 2918–2938. DOI: 10.1002/aic.10268.

[28] C. Depcik and A. Srinivasan. “One + One-Dimensional Modeling of Monolithic Catalytic Converters”. In: *Chemical Engineering Technology* 34.12 (2011), pp. 1949–1965. ISSN: 09307516. DOI: 10.1002/ceat.201100144.

[29] Anke Güthenke, Daniel Chatterjee, Michel Weibel, Bernd Krutzsch, Petr Kočí, Miloš Marek, Isabella Nova, and Enrico Tronconi. “Current status of modeling lean exhaust gas aftertreatment catalysts”. In: *Advances in Chemical Engineering*. Ed. by Guy B. Marin. Vol. 33. Academic Press, 2007, pp. 103–283. ISBN: 0065-2377. DOI: https://doi.org/10.1016/S0065-2377(07)33003-2. URL: http://www.sciencedirect.com/science/article/pii/S0065237707330032.

[30] Vladimír Novák, Petr Kočí, Tomáš Gregor, Jae-Soon Choi, František Štěpánek, and Miloš Marek. “Effect of cavities and cracks on diffusivity in coated catalyst layer”. In: *Catalysis Today* 216 (2013), pp. 142–149. ISSN: 0920-5861. DOI: https://doi.org/10.1016/j.cattod.2013.07.002. URL: http://www.sciencedirect.com/science/article/pii/S092058611300326X.

[31] James A. Dumesic. *The Microkinetics of Heterogeneous Catalysis (ACS Professional Reference Book)*. American Chemical Society, 1993. ISBN: 0841222142. URL: https://www.xarg.org/ref/a/0841222142/.

[32] I.A.W. Filot. *Introduction to microkinetic modeling*. English. Technische Universiteit Eindhoven, Dec. 2018. ISBN: 978-90-386-4520-9.

[33] Louise Olsson, Erik Fridell, Magnus Skoglundh, and Bengt Andersson. “Mean field modelling of NOx storage on Pt/BaO/Al2O3”. In: *Catalysis Today* 73.3 (2002). Environmental Catalysis, pp. 263 –270. ISSN: 0920-5861. DOI: https://doi.org/10.1016/S0920-5861(02)00009-3. URL: http://www.sciencedirect.com/science/article/pii/S0920586102000093.

[34] S. Salomons, M. Votsmeier, R.E. Hayes, A. Drochner, H. Vogel, and J. Gieshof. “CO and H2 oxidation on a platinum monolith diesel oxidation catalyst”. In: *Catalysis Today* 117.4 (2006). Selected papers presented at the 6th International Workshop on Catalytic Combustion, pp. 491 –497. ISSN: 0920-5861. DOI: https://doi.org/10.1016/j.cattod.2006.06.001. URL: http://www.sciencedirect.com/science/article/pii/S0920586106003683.

[35] Sterling E. Voltz, Charles R. Morgan, David Liederman, and Solomon M. Jacob. “Kinetic Study of Carbon Monoxide and Propylene Oxidation on Platinum Catalysts”. In: *Product RD* 12.4 (1973), pp. 294–301. ISSN: 0091-1968. DOI: 10.1021/i360048a006. URL: https://doi.org/10.1021/i360048a006.

[36] Francois Lafossas, Yoshifumi Matsuda, Ali Mohammadi, Akinori Morishima, Mikio Inoue, Maria Kalogirou, Grigorios Koltsakis, and Zissis Samaras. *Calibration and Validation of a Diesel Oxidation Catalyst Model: from Synthetic Gas Testing to Driving Cycle Applications*. 2011. DOI: https://doi.org/10.4271/2011-01-1244. URL: https://doi.org/10.4271/2011-01-1244.

[37] G.P. Ansell, P.S. Bennett, J.P. Cox, J.C. Frost, P.G. Gray, A.-M. Jones, R.R. Rajaram, A.P. Walker, M. Litorell, and G. Smedler. "The development of a model capable of predicting diesel lean NOx catalyst performance under transient conditions". In: *Applied Catalysis B: Environmental* 10.1 (1996), pp. 183 –201. ISSN: 0926-3373. DOI: https://doi.org/10.1016/0926-3373(96)00030-6. URL: http://www.sciencedirect.com/science/article/pii/0926337396000306.

[38] Timothy C. Watling, Mehrdad Ahmadinejad, Monica Ţuţuianu, Åsa Johansson, and Michael A.J. Paterson. *Development and Validation of a Pt-Pd Diesel Oxidation Catalyst Model*. 2012. DOI: https://doi.org/10.4271/2012-01-1286. URL: https://doi.org/10.4271/2012-01-1286.

[39] Marcio Schwaab and José Carlos Pinto. "Optimum reference temperature for reparameterization of the Arrhenius equation. Part 1: Problems involving one kinetic constant". In: *Chemical Engineering Science* 62.10 (2007), pp. 2750 –2764. ISSN: 0009-2509. DOI: https://doi.org/10.1016/j.ces.2007.02.020. URL: http://www.sciencedirect.com/science/article/pii/S0009250907001777.

[40] H. S. Fogler. "Chapter 18 - Models for Nonideal Reactors". In: *Elements of Chemical Reaction Engineering*. Prentice Hall PTR, 2006, pp. 848–849. ISBN: 0130473944.

[41] Enrico Tronconi and Pio Forzatti. "Adequacy of lumped parameter models for SCR reactors with monolith structure". In: 38.2 (1992), pp. 201–210. DOI: doi:10.1002/aic.690380205. URL: https://onlinelibrary.wiley.com/doi/abs/10.1002/aic.690380205.

[42] A. Holmgren and B. Andersson. "Mass transfer in monolith catalysts–CO oxidation experiments and simulations". In: *Chemical Engineering Science* 53.13 (1998), pp. 2285 –2298. ISSN: 0009-2509. DOI: https://doi.org/10.1016/S0009-2509(98)00080-3. URL: http://www.sciencedirect.com/science/article/pii/S0009250998000803.

[43] G. Groppi, W. Ibashi, M. Valentini, and P. Forzatti. "High-temperature combustion of CH4 over PdO/Al2O3: kinetic measurements in a structured annular reactor". In: *Chemical Engineering Science* 56.3 (2001), pp. 831–839. ISSN: 0009-2509. DOI: https://doi.org/10.1016/S0009-2509(00)00295-5. URL: http://www.sciencedirect.com/science/article/pii/S0009250900002955.

[44] St Walter, St Malmberg, B. Schmidt, and M. A. Liauw. "Mass transfer limitations in microchannel reactors". In: *Catalysis Today* 110.1 (2005), pp. 15–25. ISSN: 0920-5861. DOI: https://doi.org/10.1016/j.cattod.2005.09.019. URL: http://www.sciencedirect.com/science/article/pii/S0920586105006310.

[45] M. Walander, J. Sjöblom, D. Creaser, B. Lundberg, S. Tamm, and J. Edvardsson. "Efficient Experimental Approach to Evaluate Mass Transfer Limitations for Monolithic DOCs". In: *Topics in Catalysis* 62.1 (2019), pp. 391–396. ISSN: 1572-9028. DOI: 10.1007/s11244-018-1111-2. URL: https://doi.org/10.1007/s11244-018-1111-2.

[46] R. E. Hayes and S. T. Kolaczkowski. “Mass and heat transfer effects in catalytic monolith reactors”. In: *Chemical Engineering Science* 49.21 (1994), pp. 3587–3599. ISSN: 0009-2509. DOI: https://doi.org/10.1016/0009-2509(94)00164-2. URL: http://www.sciencedirect.com/science/article/pii/0009250994001642.

[47] N. Mladenov, J. Koop, S. Tischer, and O. Deutschmann. “Modeling of transport and chemistry in channel flows of automotive catalytic converters”. In: *Chemical Engineering Science* 65.2 (2010), pp. 812–826. ISSN: 0009-2509. DOI: https://doi.org/10.1016/j.ces.2009.09.034. URL: http://www.sciencedirect.com/science/article/pii/S000925090900637X.

[48] R. E. Hayes, B. Liu, and M. Votsmeier. “Calculating effectiveness factors in non-uniform washcoat shapes”. In: *Chemical Engineering Science* 60.7 (2005), pp. 2037–2050. ISSN: 0009-2509. DOI: https://doi.org/10.1016/j.ces.2004.11.041. URL: http://www.sciencedirect.com/science/article/pii/S0009250904008954.

[49] R. E. Hayes, B. Liu, R. Moxom, and M. Votsmeier. “The effect of washcoat geometry on mass transfer in monolith reactors”. In: *Chemical Engineering Science* 59.15 (2004), pp. 3169–3181. ISSN: 0009-2509. DOI: https://doi.org/10.1016/j.ces.2004.05.002. URL: http://www.sciencedirect.com/science/article/pii/S0009250904002830.

[50] Saurabh Y. Joshi, Michael P. Harold, and Vemuri Balakotaiah. “On the use of internal mass transfer coefficients in modeling of diffusion and reaction in catalytic monoliths”. In: *Chemical Engineering Science* 64.23 (2009), pp. 4976–4991. ISSN: 00092509. DOI: 10.1016/j.ces.2009.08.008.

[51] D. Papadias, L. Edsberg, and P. Björnbom. “Simplified method of effectiveness factor calculations for irregular geometries of washcoats: A general case in a 3D concentration field”. In: *Catalysis Today* 60.1 (2000), pp. 11–20. ISSN: 0920-5861. DOI: https://doi.org/10.1016/S0920-5861(00)00312-6. URL: http://www.sciencedirect.com/science/article/pii/S0920586100003126.

[52] Björn Lundberg, Jonas Sjöblom, Åsa Johansson, Björn Westerberg, and Derek Creaser. “DOC modeling combining kinetics and mass transfer using inert washcoat layers”. In: *Applied Catalysis B: Environmental* 191 (2016), pp. 116–129. ISSN: 09263373. DOI: 10.1016/j.apcatb.2016.03.024.

[53] Björn Lundberg, Jonas Sjoblom, Åsa Johansson, Björn Westerberg, and Derek Creaser. “Parameter Estimation of a DOC from Engine Rig Experiments with a Discretized Catalyst Washcoat Model”. In: *SAE International Journal of Engines* 7.2 (2014), pp. 1093–1112. ISSN: 1946-3944. DOI: 10.4271/2014-01-9049.

[54] David Kryl, Petr Kočí, Milan Kubíček, Miloš Marek, Teuvo Maunula, and Matti Härkönen. “Catalytic Converters for Automobile Diesel Engines with Adsorption of Hydrocarbons on Zeolites”. In: *Industrial Engineering Chemistry Research*

44.25 (2005), pp. 9524–9534. ISSN: 0888-5885. DOI: 10.1021/ie050249v. URL: https://doi.org/10.1021/ie050249v.

[55] Petr Kočí, Miloš Marek, Milan Kubíček, Teuvo Maunula, and Matti Härkönen. "Modelling of catalytic monolith converters with low- and high-temperature NOx storage compounds and differentiated washcoat". In: *Chemical Engineering Journal* 97.2 (2004), pp. 131–139. ISSN: 1385-8947. DOI: https://doi.org/10.1016/S1385-8947(03)00151-7. URL: http://www.sciencedirect.com/science/article/pii/S1385894703001517.

[56] A. Wheeler. "Catalysis". In: ed. by Paul H. Emmett. Vol. 2. New York: Reinhold Publishing Corporation, 1955. Chap. 2, p. 105. ISBN: 0095-9553. DOI: 10.1002/jps.3030440531. URL: https://onlinelibrary.wiley.com/doi/abs/10.1002/jps.3030440531.

[57] R. B. Evans, G. M. Watson, and E. A. Mason. "Gaseous Diffusion in Porous Media at Uniform Pressure". In: *The Journal of Chemical Physics* 35.6 (1961), pp. 2076–2083. DOI: 10.1063/1.1732211. eprint: https://doi.org/10.1063/1.1732211. URL: https://doi.org/10.1063/1.1732211.

[58] Marvin F.L. Johnson and Warren E. Stewart. "Pore structure and gaseous diffusion in solid catalysts". In: *Journal of Catalysis* 4.2 (1965), pp. 248 –252. ISSN: 0021-9517. DOI: https://doi.org/10.1016/0021-9517(65)90015-1. URL: http://www.sciencedirect.com/science/article/pii/0021951765900151.

[59] R. E. Hayes, S. T. Kolaczkowskib, P. K. C. Li, and S. Awdry. "Evaluating the effective diffusivity of methane in the washcoat of a honeycomb monolith". In: *Applied Catalysis B: Environmental* 25.2 (2000), pp. 93–104. ISSN: 0926-3373. DOI: https://doi.org/10.1016/S0926-3373(99)00122-8. URL: http://www.sciencedirect.com/science/article/pii/S0926337399001228.

[60] E. Poling Bruce, M. Prausnitz John, and P. O'Connell John. *Properties of Gases and Liquids, Fifth Edition*. 5th ed. New York: McGraw-Hill Education, 2001. ISBN: 9780070116825. URL: https://www.accessengineeringlibrary.com/content/book/9780070116825.

[61] Ramesh K. Sharma, David L. Cresswell, and Esmond J. Newson. "Effective diffusion coefficients and tortuosity factors for commercial catalysts". In: *Industrial Engineering Chemistry Research* 30.7 (1991), pp. 1428–1433. ISSN: 0888-5885. DOI: 10.1021/ie00055a004. URL: https://doi.org/10.1021/ie00055a004.

[62] D. Papadias, L. Edsberg, and P. Björnbom. "Simplified method for effectiveness factor calculations in irregular geometries of washcoats". In: *Chemical Engineering Science* 55.8 (2000), pp. 1447–1459. ISSN: 0009-2509. DOI: https://doi.org/10.1016/S0009-2509(99)00375-9. URL: http://www.sciencedirect.com/science/article/pii/S0009250999003759.

[63] D. J. Gunn. "Diffusion and chemical reaction in catalysis and absorption". In: *Chemical Engineering Science* 22.11 (1967), pp. 1439–1455. ISSN: 0009-2509. DOI:

https://doi.org/10.1016/0009-2509(67)80071-X. URL: http://www.sciencedirect.com/science/article/pii/000925096780071X.

[64] Vemuri Balakotaiah. "On the relationship between Aris and Sherwood numbers and friction and effectiveness factors". In: *Chemical Engineering Science* 63.24 (2008), pp. 5802–5812. ISSN: 00092509. DOI: 10.1016/j.ces.2008.08.025.

[65] P. Canu and S. Vecchi. "CFD simulation of reactive flows: Catalytic combustion in a monolith". In: *AIChE Journal* 48.12 (2004), pp. 2921–2935. DOI: 10.1002/aic.690481219. eprint: https://aiche.onlinelibrary.wiley.com/doi/pdf/10.1002/aic.690481219. URL: https://aiche.onlinelibrary.wiley.com/doi/abs/10.1002/aic.690481219.

[66] R. K. Shah and A. L. London. "Chapter VII - Rectangular Ducts". In: *Laminar Flow Forced Convection in Ducts*. Ed. by R. K. Shah and A. L. London. Academic Press, 1978, pp. 196–222. ISBN: 978-0-12-020051-1. DOI: https://doi.org/10.1016/B978-0-12-020051-1.50012-7. URL: http://www.sciencedirect.com/science/article/pii/B9780120200511500127.

[67] Ericson Claes, Westerberg Björn, and Odenbrand Ingemar. *A State-Space Simplified SCR Catalyst Model for Real Time Applications*. technical-paper. 2008. DOI: 10.4271/2008-01-0616. URL: http://proxy.lib.chalmers.se/login?url=http://search.ebscohost.com/login.aspx?direct=true&db=edsstp&AN=edsstp.2008.01.0616&lang=sv&site=eds-live&scope=site.

[68] L. Olsson, B. Westerberg, H. Persson, E. Fridell, M. Skoglundh, and B. Andersson. "A Kinetic Study of Oxygen Adsorption/Desorption and NO Oxidation over Pt/Al2O3 Catalysts". In: *Journal of Physical Chemistry B* 103.47 (1999). cited By 167, pp. 10433–10439. URL: https://www.scopus.com/inward/record.uri?eid=2-s2.0-0033604675&partnerID=40&md5=dcfb66ff8029ec281d5e34ce25c7bc2b.

[69] Douglas C. Montgomery. *Design and Analysis of Experiments*. Wiley, 2012. ISBN: 9781118097939. URL: https://www.xarg.org/ref/a/1118097939/.

[70] Rob J. Berger, Freek Kapteijn, Jacob A. Moulijn, Guy B. Marin, Juray De Wilde, Maria Olea, De Chen, Anders Holmen, Luca Lietti, Enrico Tronconi, and Yves Schuurman. "Dynamic methods for catalytic kinetics". In: *Applied Catalysis A: General* 342.1 (2008), pp. 3–28. ISSN: 0926-860X. DOI: https://doi.org/10.1016/j.apcata.2008.03.020. URL: http://www.sciencedirect.com/science/article/pii/S0926860X08001610.

[71] Björn Lundberg, Jonas Sjoblom, Åsa Johansson, Björn Westerberg, and Derek Creaser. "New Methodology for Transient Engine Rig Experiments for Efficient Parameter Tuning". In: *SAE International Journal of Engines* 6.4 (2013), pp. 1995–2003. ISSN: 1946-3944. DOI: 10.4271/2013-01-9043.

[72] Jazaer Dawody, Lisa Eurenius, Hussam Abdulhamid, Magnus Skoglundh, Eva Olsson, and Erik Fridell. "Platinum dispersion measurements for Pt/BaO/Al2O3, NOx storage catalysts". In: *Applied Catalysis A: General* 296.2 (2005), pp. 157 –168.

ISSN: 0926-860X. DOI: https://doi.org/10.1016/j.apcata.2005.07.060. URL: http://www.sciencedirect.com/science/article/pii/S0926860X05006332.

[73] Debbie Stokes. *Principles and Practice of Variable Pressure / Environmental Scanning Electron Microscopy (VP-ESEM)*. Wiley, 2008. ISBN: 0470065400. URL: https://www.xarg.org/ref/a/0470065400/.

[74] Tomáš Starý, Olga Šolcová, Petr Schneider, and Miloš Marek. "Effective diffusivities and pore-transport characteristics of washcoated ceramic monolith for automotive catalytic converter". In: *Chemical Engineering Science* 61.18 (2006), pp. 5934–5943. ISSN: 00092509. DOI: 10.1016/j.ces.2006.05.014.

[75] Douglas M. Ruthven. "Diffusion in type A zeolites: New insights from old data". In: *Microporous and Mesoporous Materials* 162 (2012), pp. 69–79. ISSN: 13871811. DOI: 10.1016/j.micromeso.2011.12.025.

Nomenclature

Abbreviation	Description
ASC	Ammonia Slip Catalyst
CFD	Computational Fluid Dynamics
CPSI	Cells Per Square Inch
CRT	Continuously Regenerating Trap
CSTR	Continuously Stirred Tank Reactor
DPF	Diesel Particulate Filter
DOC	Diesel Oxidation Catalyst
DoE	Design of Experiments
EATS	Exhaust Aftertreatment System
EU	European Union
GA	Gravimetric Analysis
HC	Hydrocarbons
ICE	Internal Combustion Engine
IGA	Intelligent Gravimetric Analysis
LNT	Lean NOx Trap
MFC	Mass Flow Controller
NO_X	Nitrogen oxides
NSR	NOx Storage and Reduction
OECD	Organisation for Economic Co-operation and Development
PFR	Plug Flow Reactor
PM	Particulate Matter
POCS	Periodic Open Cellular Substrates
SCAT	Synthetic Catalyst Activity Test
SCR	Selective Catalytic Reduction
SEM	Scanning Electron Microscopy
TPD	Temperature Programmed Desorption
WHO	World Health Organization

Variables	Description
A_j	Pre-exponential factor
A_k	Wetted area in tank k
$c_{i,k,n}$	Concentration
D_{AB}	Molecular Diffusivity of species A in B
d_H	Hydraulic diameter
d_μ	Average micro pore diameter
d_M	Average macro pore diameter
d_{wsc}	Washcoat thickness
$Deff$	Effective diffusivity
Ea_j	Activation Energy
F_{tot}	Total molar flow rate in gas phase
kc	External mass transfer coefficient
$k_{j,k,n}$	Reaction rate constant
l	Length scale
$m_{k,n}$	Mass of catalyst
$Nu_{\infty,T}$	Asymptotic Nusselt number
R	Gas constant
R_{bulk}	Characteristic dimension of the open channel
$r_{j,k,n}$	Reaction rate
R_{wsc}	Characteristic dimension of the washcoat
Sh_z	Axially resolved Sherwood number
Sh_∞	Asymptotic Sherwood number
t	Time
t_c	Residence time scale
t_r	Reaction time scale
T_{ref}	Reference temperature
t_{td}	Transverse diffusion time scale
t_{wd}	Washcoat diffusion time scale
v	Fluid velocity
$v_{i,j}$	Stoichiometric coefficient
$V_{k,n}$	Volume for a tank
$y_{i,k,n}$	Gas phase molar fraction
z^*	Dimensionless axial coordinate

Greek characters	**Description**
Δx_k	Distance between tanks
$\Gamma_{i,k,n}$	Mass transfer coefficient
λ	Mean free path

Subscripts and indices	**Description**
i	Species
j	Reaction
k	Tank
n	Layer

Substances	**Description**
C_3H_6	Hexane
CO	Carbon monoxide
CO_2	Carbon dioxide
H_2O	Water
HC	Hydrocarbons
N_2	Nitrogen
NH_3	Ammonia
NO	Nitrogen monoxide
NO_2	Nitrogen dioxide
NO_X	Nitrogen oxides (grouping)
SO_2	Sulfur dioxide

List of Figures

List of Tables